Available online at www.sciencedirect.com
ScienceDirect
Journal of Catalysis 245 (2007) 35–44
JOURNAL OF CATALYSIS
www.elsevier.com/locate/jcat

Low-temperature catalytic carbon monoxide oxidation over hydrous and anhydrous palladium oxide powders

Seung-Hoon Oh, Gar B. Hoflund *

Department of Chemical Engineering, University of Florida, Gainesville, FL 32611, USA

Received 13 July 2006; revised 11 September 2006; accepted 17 September 2006

Available online 19 October 2006

Abstract

Low-temperature CO oxidation was carried out over hydrous and anhydrous PdO powders to examine the effects of surface water species. Hydrous PdO exhibits 100% CO conversion even at room temperature, whereas hydrous PdO pretreated in He at 400 °C and anhydrous PdO do not exhibit significant CO oxidation activity even at 100 °C. Approximately one-half of the CO is oxidized catalytically over hydrous PdO by gas-phase oxygen, whereas oxygen contained in the solid oxidizes the rest of the CO by a gas–solid reaction. X-ray photoelectron spectroscopy (XPS) data indicate that the water is present in hydrous PdO as hydroxyl groups and not molecular water. Without the presence of these hydroxyl groups, CO oxidation does not occur. During CO oxidation, metallic Pd forms and hydroxyl groups may react to form water, resulting in significant activity decay. The metallic Pd is inactive for catalytic CO oxidation at the temperatures used in this study. As the reaction temperature is increased from 30 to 100 °C, subsurface hydroxyl groups migrate to the surface, partially restoring the catalytic activity.
© 2006 Elsevier Inc. All rights reserved.

Keywords: Catalytic CO oxidation; Low-temperature CO oxidation; Hydrous PdO; Anhydrous PdO; X-ray photoelectron spectroscopy; Stoichiometric CO and O_2

1. Introduction

Palladium-containing catalysts are widely used for oxidation reactions including the complete oxidation of methane, automotive exhaust treatment, and CO oxidation [1–9]. Although oxide–supported platinum and gold catalysts [10–19] are generally more active for low-temperature (<100 °C) CO oxidation than oxide–supported palladium catalysts, Pd-containing catalysts are used for this reaction [4,5,20–23]. The supported catalysts used for low-temperature CO oxidation are quite complex; thus, determining how they function has been difficult, even though CO oxidation is a relatively simple catalytic reaction. Pd supported on different oxide powders gives different catalytic behavior for both CO oxidation [12] and methane oxidation [24], indicating that the support–metal or support–oxide interaction is important for oxide–supported Pd catalysts in oxidation reactions.

The purpose of this study was to simplify the catalytic process as much as possible to gain information about the catalytically active phase of Pd, the influence of surface water and hydroxyl groups, and the mechanism of CO oxidation. In a previous study, H_2-reduced Pd metal powder was studied for CO oxidation [25]. The reaction feed contained both CO and O_2 and thus was both reducing and oxidizing. With a slightly O_2-rich (∼150 ppm) feed stream, PdO formed at the surface at 50–300 °C, according to X-ray photoelectron spectroscopy (XPS) data. This PdO was the catalytically active phase for CO oxidation under the conditions used. Because reduction in H_2 was performed, Pd hydride may have been the starting material, and a high concentration of hydroxyl groups likely was present on these surfaces. Catalytic CO oxidation did not occur over Pt and Pd at low temperatures because CO covered the surface, leaving no sites for chemisorption of oxygen. In the case of platinized tin oxide, Hoflund et al. [26] found that a Pt/Sn alloy provided a two-site surface over which low-temperature CO oxidation occurred. They proposed a mechanism in which bicarbonate or formate species are the reaction intermediates formed by reaction with surface hydroxyl species [27]. These hydroxyl species

* Corresponding author. Fax: +1 352 392 9513.
E-mail address: garho@hotmail.com (G.B. Hoflund).

0021-9517/$ – see front matter © 2006 Elsevier Inc. All rights reserved.
doi:10.1016/j.jcat.2006.09.016

have been observed using XPS on catalytically active platinized tin oxide surfaces [13].

Based on these results, this present study of CO oxidation was carried out over anhydrous PdO powder, anhydrous PdO powder that had been exposed to humid air for about 1 year, and hydrous PdO. The reaction and XPS data obtained provide information about the role of water or hydroxyl groups in low-temperature CO oxidation, the catalytically active species, and the mechanism.

2. Experimental

Hydrous palladium (II) oxide ($PdO{\cdot}0.8H_2O$, Pd 77.81%, purity 99.9% Alfa Aesar), air-exposed anhydrous palladium (II) oxide (PdO, Pd 86.80%, purity 99.9%, Alfa Aesar) and fresh, Ar-sealed anhydrous palladium (II) oxide (PdO, purity 99.998%, Aldrich) were examined. Two anhydrous PdO powders from different sources were used to ensure that the results do not depend on sample source or minor differences in impurity levels. A specific mass (100 or 400 mg) of palladium oxide was loaded into a 1/4-inch-diameter, U-shaped quartz tube and supported by glass wool. The BET surface area was 35.7 m^2/g for hydrous PdO, 28.9 m^2/g for air-exposed anhydrous PdO, and 30.2 m^2/g for anhydrous PdO. The tube was then inserted into a Thermolyne 21100 furnace. A K-type thermocouple was placed around the U-tube at the center of the catalyst bed and connected to an autotuning PID controller. The temperature was increased at a rate of 10 °C/min from room temperature to 100 °C in flowing He and maintained accurately inside the furnace within ±1 °C. Ultra-high-purity test gases obtained from Praxair were mixed to yield a composition close to 1.0% CO and 0.50% O_2 in helium. Because it is not possible to maintain a stoichiometric feed stream due to mass controller fluctuations, the feed stream was maintained slightly oxygen rich by <200 ppm. The total flow rate was 45 cc/min at STP. Initially, a pure He flush gas was passed through the catalyst bed for 5 min. The feed gas mixture was bypassed and analyzed in a Hewlett Packard 5890A gas chromatograph to determine the feed concentration. For product analysis, a molecular sieve 5A column was connected to a thermal conductivity detector (TCD). The oven and TCD temperatures were kept essentially constant at 80 and 150 °C, respectively.

Surface characterization studies were carried out on the catalysts before and after reaction at various temperatures. The catalyst powders were thoroughly mixed, pressed into aluminum cups, inserted into the ultra-high-vacuum chamber, and characterized by XPS. The bed lengths were 5 mm for the 100-mg sample and 20 mm for the 400-mg sample. There may have been catalyst surface compositional differences across the bed. By thoroughly mixing the used powders, an average composition was obtained using XPS. XPS was performed using a double-pass cylindrical mirror analyzer (DPCMA, PHI model 25-255 AR) and pulse-counting detection [28] by operating the DPCMA in the retarding mode, with a pass energy of 25 eV for the narrow-range spectra and 50 eV for the survey spectra. The X-rays were generated using a Mg$K\alpha$ X-ray source. The raw spectra were shifted to align the predominant PdO Pd $3d_{5/2}$ peak, with the accepted binding energy (BE) of 336.9 eV. No charging problems were encountered in this study. Model experiments were performed to ensure that the brief exposure to air during the transfer from the catalytic reactor to the characterization chamber did not alter the Pd chemical state. The Pd powder was fully reduced in the reactor, exposed to air for 1 h, and analyzed using XPS. Only Pd metal was observed. In another experiment, both hydrous and anhydrous PdO were partially reduced in the UHV system. XPS was performed, the samples were exposed to air for 1 h, and then XPS was performed again. The spectra taken before and after the air exposure were identical, indicating that Pd metal was not oxidized and water was not adsorbed by this air exposure at room temperature.

3. Results and discussion

Three different powders were examined in this study: a hydrous PdO powder, an anhydrous PdO powder that had been exposed to humid air for about 1 year, and an anhydrous PdO powder taken directly from a sealed bottle and stored in a desiccator. XPS Pd 3d spectra obtained from these three powders are shown in Fig. 1, and the corresponding XPS O 1s and Pd $3p_{3/2}$ spectra are shown in Fig. 2. In Fig. 1, the primary difference is in the FWHM of the Pd 3d peaks. The fresh anhydrous PdO has the smallest FWHM (1.73 eV), and the hydrous PdO has the largest FWHM (1.96 eV). The larger FWHM obtained from hydrous PdO indicates an electronic interaction between the lattice water species and PdO. The air-exposed, anhydrous PdO has a slightly larger FWHM than that of fresh anhydrous PdO, suggesting that only a small amount of water was adsorbed at the surface during the long-term exposure to moist air.

The corresponding O 1s and Pd 3p spectra shown in Fig. 2 exhibit much larger differences than the Pd 3d spectra shown in Fig. 1. However, these spectra are considerably more complicated, because they contain contributions from multiple species.

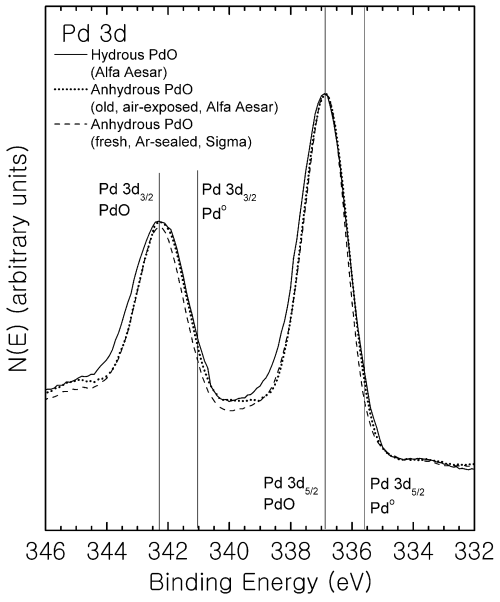

Fig. 1. XPS Pd 3d spectra obtained from fresh hydrous PdO, air-exposed anhydrous PdO and argon-sealed anhydrous PdO.

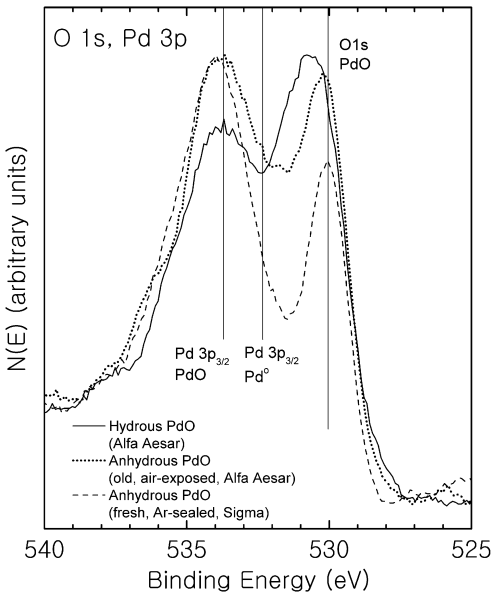

Fig. 2. XPS O 1s and Pd 3p spectra obtained from fresh hydrous PdO, air-exposed anhydrous PdO and argon-sealed anhydrous PdO.

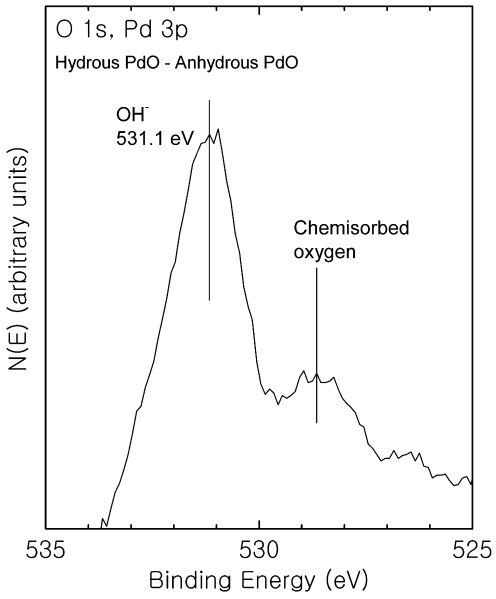

Fig. 3. XPS O ls and Pd 3p difference spectrum obtained by subtracting the anhydrous PdO spectrum shown in Fig. 2 from the hydrous PdO spectrum also shown in Fig. 2.

Table 1
XPS peak binding energy assignments

Species	Peak	BE (eV)	References
Pd^0	Pd $3d_{5/2}$	335.3	[25,29]
	Pd $3p_{3/2}$	532.3	[25]
PdO	Pd $3d_{5/2}$	336.9	[25,29]
	Pd $3p_{3/2}$	533.7	[25,29]
	O 1s	530.1	[25,29]
$Pd(OH)_2$	Pd $3d_{5/2}$	336.9	This study
	Pd $3p_{3/2}$	533.7	This study
	O 1s	531.1	This study, [27,30,31]
H_2O	O 1s	533.0	[30,31]

Peak BE assignment used in this study are given in Table 1; they are quite close to the reference literature values. Lines are drawn at the BEs of Pd $3p_{3/2}$ in PdO, Pd $3p_{3/2}$ in Pd metal, and O 1s in PdO. No contributions from Pd metal are present in these spectra based on the spectra shown in Fig. 1. The spectrum obtained from fresh anhydrous PdO is characteristic of that of anhydrous PdO, containing a well-defined O 1s peak due to O in PdO and a Pd $3p_{3/2}$ peak due to Pd in PdO. The spectrum obtained from hydrous PdO is very different. Contributions from O in PdO and Pd in PdO are apparent, but a large contribution due to incorporated lattice water species is present between 530 and 533 eV. The nature of the incorporated lattice water species is discussed below. The spectrum obtained from the air-exposed anhydrous PdO exhibits a Pd $3p_{3/2}$ peak due to PdO and an O 1s peak due to PdO. It also exhibits structure between 530 and 533 eV due to exposure to humid air, but this structure is much smaller than that of hydrous PdO. The O 1s and Pd $3p_{3/2}$ spectra in Fig. 2 are consistent with the data in Fig. 1 but are much more sensitive to incorporated surface water species. The difference between the O 1s and Pd 3p spectra obtained from hydrous PdO and the fresh anhydrous PdO is the contribution due to incorporated water. This difference spectrum, shown in Fig. 3, consists of a fairly narrow peak with a BE of 531.1 eV. This is lower than the accepted BEs for water by about 2 eV [30,31] but is typical of hydroxyl groups [27,30–32]. This suggests that the formula of hydrous PdO ($PdO{\cdot}H_2O$) is $Pd(OH)_2$. The actual formula of this powder is $PdO{\cdot}0.8H_2O$, indicating that some PdO is also present in this powder. Apparently no information on $Pd(OH)_2$ is available in the literature. The small feature at 528.7 eV is assigned as chemisorbed atomic O. A similar species has been observed in a Ag oxide study [33] and in a study of surface and subsurface oxygen on Pd(111) [34].

The catalytic activity of 100 mg of hydrous PdO for CO oxidation as a function of time at 100 °C is shown in Fig. 4. The feed gas was 1.0% CO and 0.51% O_2. Complete CO conversion was obtained over 30 min with an oxygen conversion of only 46–52% for this period. For the catalytic reaction between gas-phase CO and O_2, 100% CO conversion required almost 100% O_2 conversion for the feed ratio used. The fact that the O_2 conversion is about 50% indicates that oxygen from the hydrous PdO reacted with CO to produce CO_2 at 100 °C. Specifically, this oxygen must come from the PdO or hydroxyl groups, or both sources. When pure Pd metal was tested with 1% CO and 0.51% O_2 in He at 300 °C [25], complete conversion of CO and nearly complete conversion of O_2 were achieved. After 33 min, the activity of hydrous PdO gradually decreased over the next 60 min and then became negligible. The O_2 conversion remains at approximately 50% of the CO conversion until both conversions become negligible.

To determine the effect of hydroxyl groups in hydrous PdO on catalytic activity, 100 mg of fresh hydrous PdO was pretreated by drying in He at 400 °C for 1 h, then cooled to 100 °C in flowing He. The reaction-gas feed stream for the 400 °C—calcined hydrous PdO was slightly O_2-rich (1.0% CO

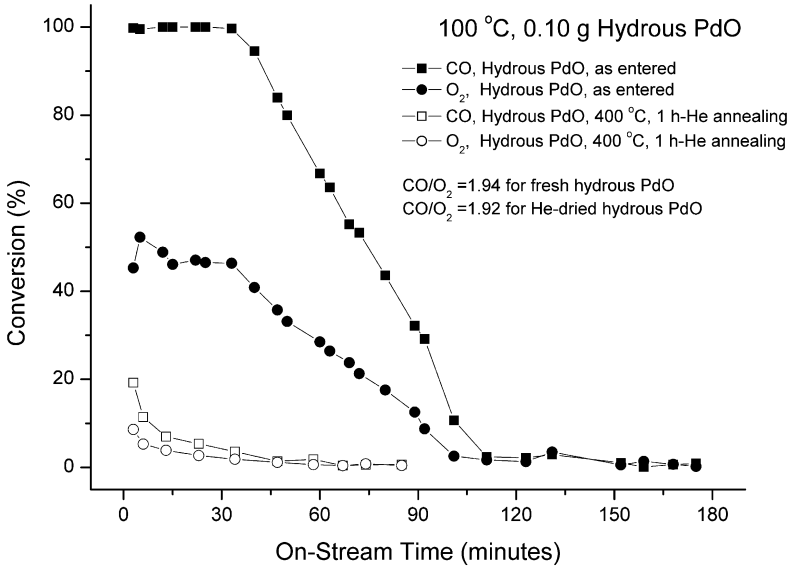

Fig. 4. Comparison of CO and O_2 conversions as a function of reaction time over 100 mg of hydrous PdO at 100 °C before and after annealing in He at 400 °C for 1 h. The feedstreams were slightly oxygen rich (1.0% CO and 0.51% O_2 without annealing in He and 1.0% CO and 0.52% O_2 with annealing in He) at total flow rates of 45 cc/min.

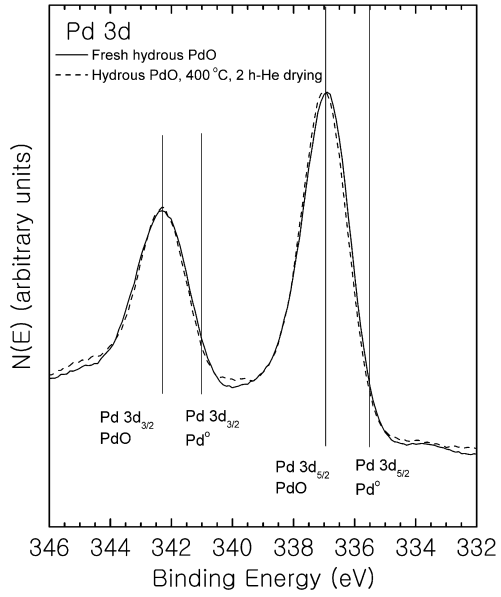

Fig. 5. XPS Pd 3d spectra obtained from fresh hydrous PdO, hydrous PdO after drying in He at 150 °C for 120 min in the reactor and hydrous PdO after drying in He at 400 °C for 120 min in the reactor.

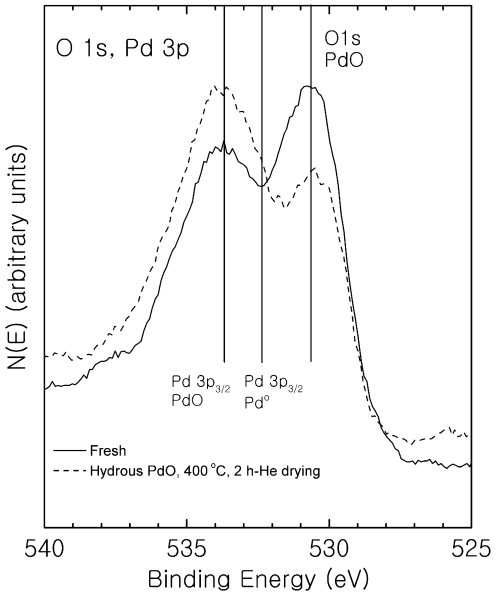

Fig. 6. XPS O 1s and Pd 3p spectra obtained from fresh hydrous PdO, hydrous PdO after drying in He at 150 °C for 120 min in the reactor and hydrous PdO after drying in He at 400 °C for 120 min in the reactor.

and 0.52% O_2). The initial CO conversion of the dried hydrous PdO was 20%, whereas the O_2 conversion was only 10%. CO conversion decreased to <5% after 30 min of reaction time. Although the conversions were very low after the drying treatment, the O_2 conversion was still about one-half of the CO conversion.

XPS Pd 3d spectra obtained from fresh hydrous PdO and hydrous PdO pretreated in He at 400 °C for 2 h are shown in Fig. 5. In both cases, the predominant peaks are due to PdO or hydroxide, and no feature due to metallic Pd is apparent. The spectrum obtained from the fresh, hydrous PdO is slightly broader than those obtained from the 400 °C annealed sample, indicating that annealing removes hydroxyl groups from hydrous PdO by a solid-phase reaction that forms PdO and H_2O from $Pd(OH)_2$. This is consistent with the catalytic results shown in Fig. 4. These peaks are not as narrow as those obtained from anhydrous PdO, most likely because a defect structure remains after annealing at 400 °C. The corresponding high-resolution XPS O 1s and Pd $3p_{3/2}$ spectra are shown in Fig. 6. Comparing these spectra with those in Fig. 2 indicates that annealing results in desorption of water from the hydrous PdO. After annealing at 400 °C in He for 2 h, the spectrum approaches that obtained from fresh anhydrous PdO but with some surface and/or subsurface hydroxyl groups still present, because the valley between two predominant peaks is not as deep.

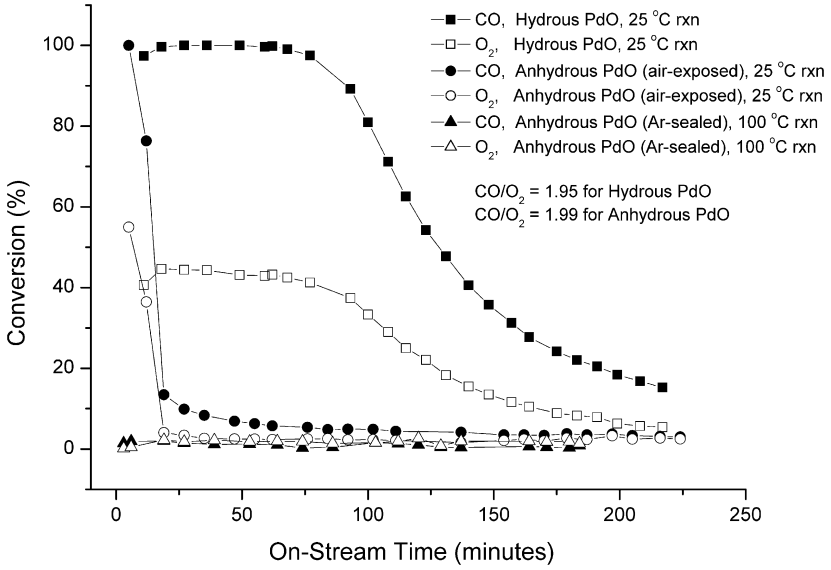

Fig. 7. Comparison of CO and O_2 conversions as a function of reaction time at 25 °C over 400 mg of hydrous PdO, air-exposed anhydrous PdO and at 100 °C over 100 mg of argon-sealed anhydrous PdO. The feedstreams were slightly O_2 rich (1.0% CO and 0.51% O_2 for hydrous PdO and 1.0% CO and 0.502% O_2 for air-exposed anhydrous PdO and argon-sealed anhydrous PdO) at a total flow rate of 45 cc/min.

The CO and O_2 conversions obtained at room temperature from hydrous PdO and air-exposed anhydrous PdO are compared in Fig. 7. Fresh hydrous PdO (0.40 g) was exposed to a flow rate of 45 cc/min of 1.0% CO and 0.52% O_2 in He at 25 °C. Complete CO conversion was maintained over 75 min while the O_2 conversion ranged from 41 to 44% of the CO conversion over the same time period. After this period, the CO activity decreased with reaction time until a CO conversion of 15% was reached after 217 min. Air-exposed anhydrous PdO (0.40 g) was also exposed to a flow rate of 45 cc/min of 1.0% CO and 0.51% O_2 in He at 25 °C. For a short period (<12 min), air-exposed anhydrous PdO also exhibited high CO conversion (initially 100%). However, it rapidly deactivated and yielded 13% CO conversion after 19 min. The activity then decayed slowly to a few percent. The oxygen conversion was initially 55% and decreased to 36% at 12 min, which are about one-half of the corresponding CO conversions. The unusually high initial activity of air-exposed anhydrous PdO is due to accumulation of hydroxyl groups at the surface during exposure to moist air over a long period. Fresh anhydrous PdO exhibited no CO oxidation activity even at 100 °C, as shown in Fig. 7.

The XPS spectra shown in Figs. 8 and 9 were obtained from hydrous PdO after reaction for 30 and 220 min, respectively (0.40 g, slightly O_2-rich feed and 25 °C). Metallic Pd features form during reaction. After 30 min of reaction, they are small shoulders on the low-BE side of the Pd 3d peaks, but after 220 min of reaction, they are quite prominent. At this time, almost 40% of the near-surface $Pd(OH)_2$ and PdO are converted to Pd metal. The O 1s feature obtained after reaction for 30 min (Fig. 9) is similar to that obtained from fresh hydrous PdO, as expected, but it is significantly decreased after 220 min of reaction. These spectra are normalized to allow comparison of their structures. As oxygen is removed during reaction, the Pd feature becomes predominant in the normalized spectra. Increased structure is present in the metallic Pd $3p_{3/2}$ region after 30 min

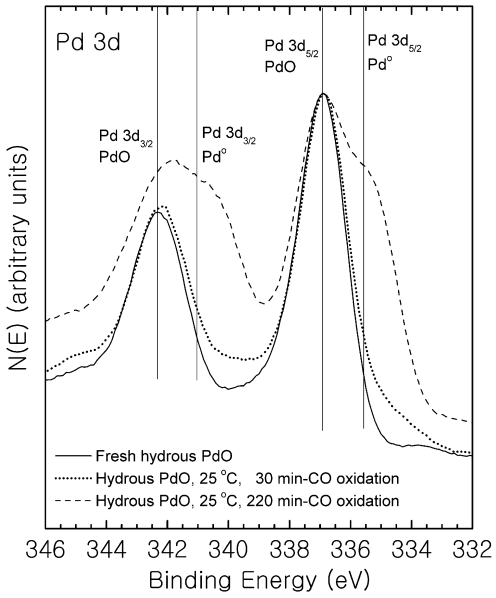

Fig. 8. XPS Pd 3d spectra obtained from fresh hydrous PdO, hydrous PdO after exposure to 1.0% CO and 0.51% O_2 for 30 min in the catalytic reactor at 25 °C and hydrous PdO after exposure to 1.0% CO and 0.51% O_2 for 220 min in the catalytic reactor at 25 °C.

of reaction and even more so after 220 min of reaction as PdO is converted to metallic Pd. These spectra are complex because the lattice hydroxyl group content also decreases with reaction time.

The effect of reaction temperature for CO oxidation over hydrous PdO is shown in Fig. 10. At 100 °C, complete CO conversion and nearly 42% O_2 conversion are maintained for 170 min. At 25 °C, complete CO conversion is maintained for only about 65 min, and again the O_2 conversion is slightly less than one-half of the CO conversion over the time period studied. This behavior implies that less than one-half of the oxygen

in the feed gas is participating in CO oxidation, so the rest of the required oxygen comes from PdO and/or $Pd(OH)_2$. According to the XPS data shown in Figs. 8 and 9, when hydrous PdO is no longer active for CO oxidation, most of the near-surface PdO and/or $Pd(OH)_2$ is converted into Pd metal, and the near-surface hydroxyl groups are depleted. The conversion remains high longer at 100 °C than at 25 °C. This implies that subsurface hydroxyl groups migrate to the surface faster at 100 °C to maintain the high activity. The corresponding Pd 3d features and Pd 3p/O 1s features are shown in Figs. 11 and 12, respectively, before and after reaction at 25 °C for 220 min and 100 °C for 205 min. These data indicate that Pd metal forms more rapidly at higher reaction temperatures even though the catalyst still exhibits 60% CO conversion before the XPS data are obtained. The O 1s and Pd $3p_{3/2}$ spectra shown in Fig. 12 also indicate that oxygen is removed from the near-surface region by the decreased size of the O 1s peak. This decrease is larger after reaction at 100 °C than after reaction at 25 °C, consistent with the Pd 3d spectra shown in Fig. 11. The feature due to O in PdO is diminished simultaneously as the peak due to metallic Pd grows.

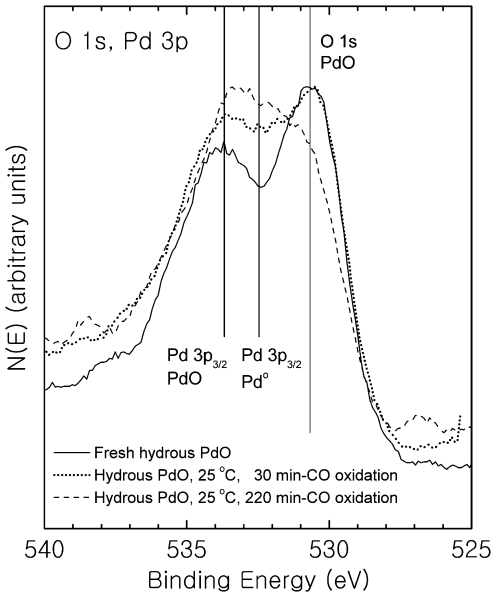

Fig. 9. XPS O 1s and Pd 3p spectra obtained from fresh hydrous PdO, hydrous PdO after exposure to 1.0% CO and 0.51% O_2 for 30 min in the catalytic reactor at 25 °C and hydrous PdO after exposure to 1.0% CO and 0.51% O_2 for 220 min in the catalytic reactor at 25 °C.

Next, 400 mg of fresh hydrous PdO was reacted with 1% CO (no O_2 in the feed gas) at 25 °C. The data shown in Fig. 13 indicate that hydrous PdO reacts with CO molecules even at 25 °C, exhibiting a maximum CO conversion of ∼97% for 20 min before gradually decreasing. The same experiment was also carried out with 0.51% O_2 in the feed. Comparing the two conversions versus time curves, the conversion without O_2 deactivates faster and exhibits lower CO conversion over the entire reaction time. The area between the two curves is proportional to the amount of O_2 that reacts catalytically from the gas phase.

The conversions of CO and O_2 over 1.0% CO and 0.503% O_2 in He (45 cc/min) over 400 mg of hydrous PdO at increasing reaction temperatures are shown in Fig. 14. At 25 °C, hydrous PdO exhibits 100% CO conversion and 44% O_2 conversion for 60 min before gradually deactivating to CO conversion of 15% and O_2 conversion of 5% at 220 min. The reaction temperature was then increased to 70 °C. At this temperature, the initial CO conversion is 100%, whereas the O_2 conversion is <13%. The low O_2 conversion at 70 °C indicates that O_2 in the feed gas does not react to a significant extent, so more oxygen from the solid reacts with CO for a short period. At 100 °C, an initial 36% CO conversion is found, with no reaction of oxygen in the feed stream. The CO conversion decreases rapidly to a few percent at about 65 min. As the reaction proceeds at each temperature, the surface becomes more reduced, and consequently the conversion decreases. When the temperature is increased, more hydroxyl groups diffuse to the surface from the subsurface

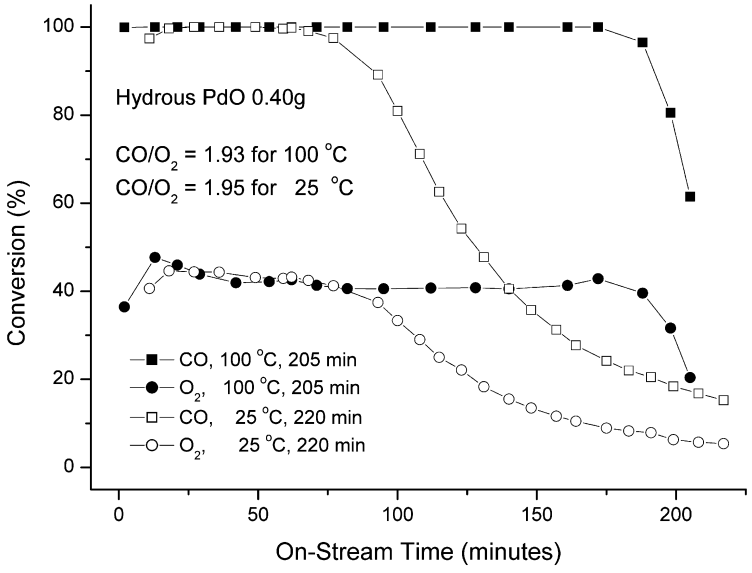

Fig. 10. CO and O_2 conversions as a function of reaction time over 400 mg of hydrous PdO at 100 °C for 205 min and 25 °C for 217 min. The feedstreams contained 1.0% CO and 0.52% O_2 at 100 °C and 1.0% CO and 0.51% O_2 at 25 °C. The total flow rate was 45 cc/min.

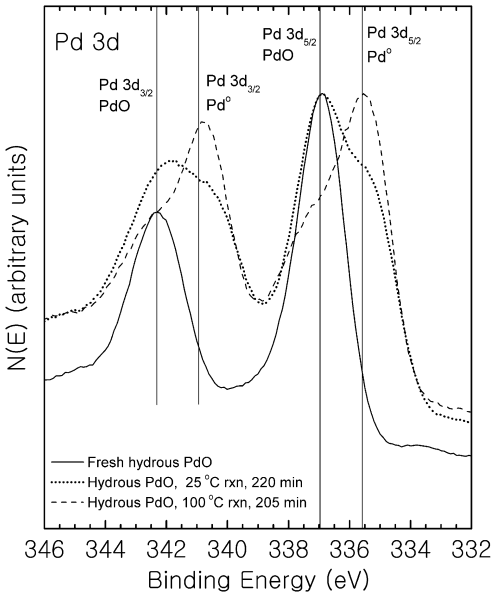

Fig. 11. XPS Pd 3d spectra obtained from fresh hydrous PdO, hydrous PdO after exposure to 1.0% CO and 0.51% O_2 for 220 min in the catalytic reactor at 25 °C and hydrous PdO after exposure to 1.0% CO and 0.52% O_2 for 205 min in the catalytic reactor at 100 °C.

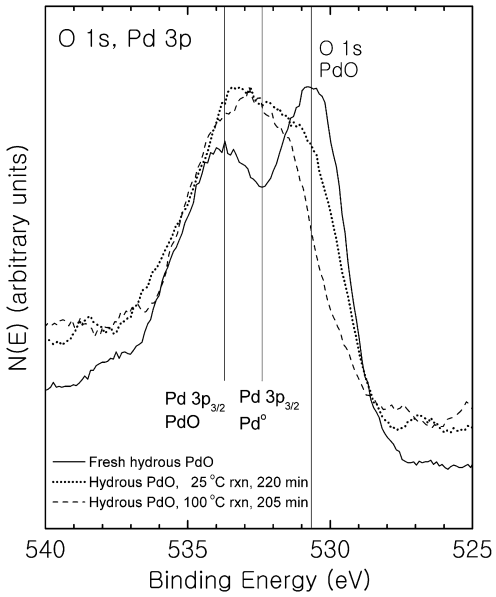

Fig. 12. XPS O 1s and Pd 3p spectra obtained from fresh hydrous PdO, hydrous PdO after exposure to 1.0% CO and 0.51% O_2 for 220 min in the catalytic reactor at 25 °C and hydrous PdO after exposure to 1.0% CO and 0.52% O_2 for 205 min in the catalytic reactor at 100 °C.

region, yielding a high CO conversion. The high conversion period becomes shorter as the near-surface region becomes more fully reduced to Pd metal. The Pd metal at the surface is covered by chemisorbed CO at these temperatures, so gas-phase oxygen cannot adsorb and react.

The CO conversion comparison for hydrous PdO (0.40 g) with no O_2 added to the feed is also shown in Fig. 14. The CO conversion without O_2 in the feed exhibits lower CO conversion and faster deactivation for the entire reaction time at all temperatures. Without O_2, hydrous PdO yields a 9% CO conversion after 216 min at 25 °C. The activity increases to CO conversions of 86% at 70 °C and 36% at 100 °C. The area between the curves (open circles and open squares) represents the amount of O_2 from the feed stream that is reacted.

XPS spectra obtained from hydrous PdO reacted with and without O_2 in the feed stream for more than 6 h at 25, 70, and 100 °C are shown in Figs. 15 and 16. The XPS Pd 3d spectra indicate that the chemical state of Pd in hydrous PdO changes to metallic Pd during reaction in both cases. This alteration occurs more rapidly without the presence of O_2 in the feed stream, as expected. The XPS O 1s and Pd $3p_{3/2}$ features (Fig. 16) behave in a manner consistent with the XPS Pd 3d spectra; the O 1s feature in PdO is diminished in size, and the Pd $3p_{3/2}$ feature is

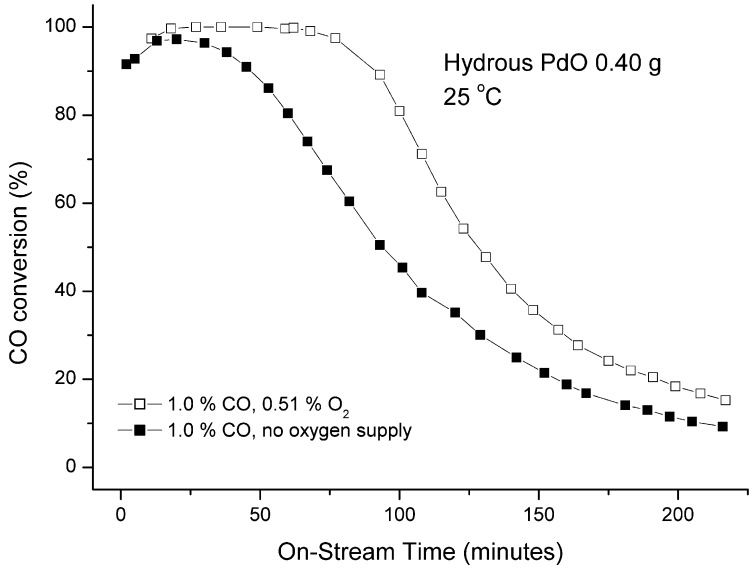

Fig. 13. CO conversion as a function of reaction time at 25 °C over 400 mg of hydrous PdO in 1.0% CO and 0.51% O_2 in He and 1.0% CO only (no O_2) in He both at a total flow rate of 45 cc/min.

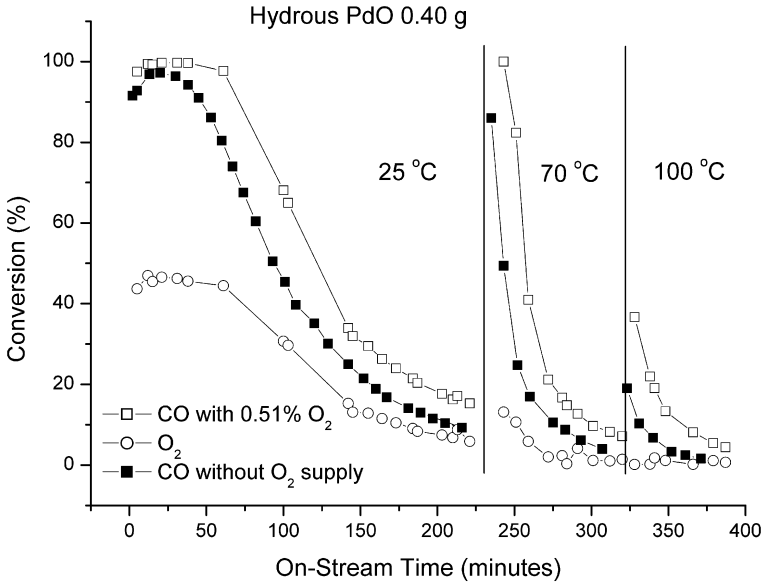

Fig. 14. CO (open square) and O_2 (open circle) conversions as a function of reaction time over 400 mg of hydrous PdO at 25 °C (216 min), 70 °C (77 min), and 100 °C (59 min). The feedstream contained 1.0% CO and 0.503% O_2 in He at a total flow rate of 45 cc/min. CO conversion (solid squares) is also shown as a function of reaction time at 25 °C (216 min), 70 °C (70 min), and 100 °C (66 min). The feedstream contained 1.0% CO only (no oxygen) in He in this case. The total flow rate was 45 cc/min.

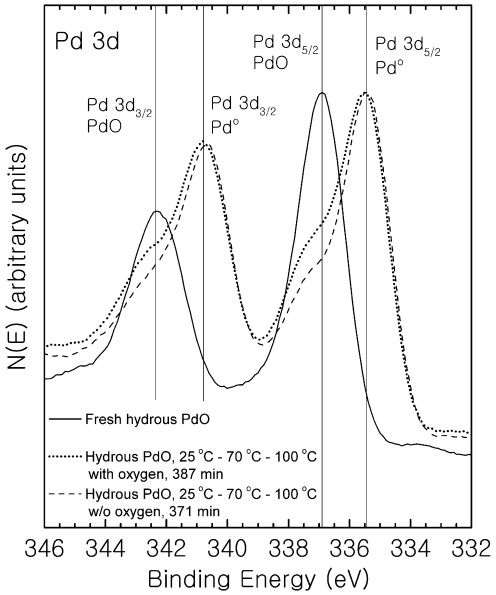

Fig. 15. XPS Pd 3d spectra obtained from fresh hydrous PdO, hydrous PdO after exposure to 1.0% CO and 0.51% O_2 in He at the end of the temperature–time program described in Fig. 10 and hydrous PdO after exposure to 1.0% CO only in He at the end of the temperature–time program described in Fig. 14.

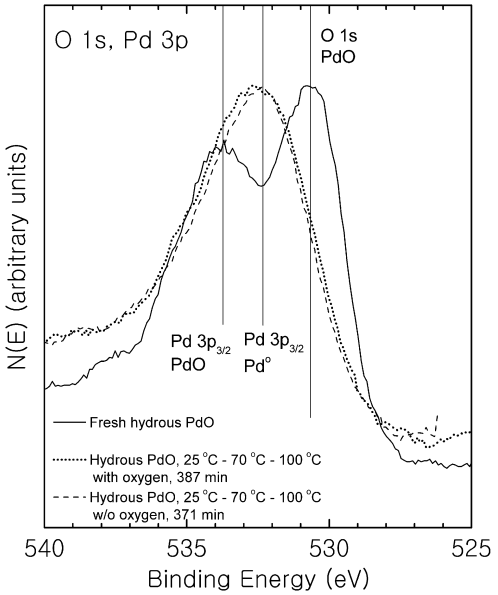

Fig. 16. XPS O 1s and Pd 3p spectra obtained from fresh hydrous PdO, hydrous PdO after exposure to 1.0% CO and 0.51% O_2 in He at the end of the temperature–time program described in Fig. 10 and hydrous PdO after exposure to 1.0% CO only in He at the end of the temperature–time program described in Fig. 14.

shifted to that of metallic Pd. These changes occur to a greater extent for the catalyst run without O_2 in the feed stream.

An explanation for the conversion data shown in Fig. 14 can be based on the XPS data shown in Figs. 15 and 16. As reaction occurs at 25 °C with oxygen in the feed, PdO and $Pd(OH)_2$ are reduced to Pd metal, and H_2O may be lost to the gas phase. These processes result in decreasing conversion. When the temperature is increased to 70 °C, subsurface oxygen migrates to the surface, where it reacts with CO. The surface is less active catalytically, as indicated by the fact that only a small amount of gas-phase oxygen reacts. At 100 °C, no gas-phase oxygen reacts with CO, so the CO that is oxidized reacts only with oxygen or hydroxyl groups that migrate to the surface. These data demonstrate that metallic Pd is not a catalytically active phase under the reaction conditions used in this study. This is consistent with a previous study [25] demonstrating that metallic Pd powder exhibits no catalytic activity for CO oxidation below 170 °C.

The argument can be made that H_2O is present in hydrous PdO as hydroxyl groups based on a connection between the re-

action data and the XPS data. For the conversion data obtained using hydrous PdO at 100 °C (Fig. 4, solid symbols), 9.24×10^{20} molecules of CO are converted to CO_2 over 120 min. This requires 4.62×10^{20} molecules of O_2. The oxygen in the feed stream contributes 2.14×10^{20} molecules, so 4.96×10^{20} O atoms from the solid phase must react, which is 1.4×10^{16} O atoms/cm^2 based on a surface area of 35.7 m^2/g and a sample size of 100 mg. If a $PdO{\cdot}H_2O$ composition with a layer atom density of 1×10^{15} atoms/cm^2 were assumed and only O from H_2O reacted with CO, then the XPS Pd 3d features shown in Fig. 11 would exhibit no metallic character, which clearly is not the case. If only O in PdO reacts, then metallic Pd forms. The H_2O either remains dissolved in metallic Pd in the top 42 atomic layers, which is not plausible, or it desorbs. This is deeper than the detection depth of XPS [35], so only metallic Pd should be apparent in the XPS Pd 3d spectrum. This also is not the case. If the oxygen in both PdO and assumed H_2O reacted, then 21 atomic layers would be reduced to Pd metal. XPS probes more deeply than this, so underlying PdO would be apparent in addition to a larger metallic Pd feature. This is the case shown in Fig. 11. Therefore, both forms of oxygen are equivalent in terms of CO oxidation. This supports the finding described above that $PdO{\cdot}0.8H_2O$ is actually a mixture of $Pd(OH)_2$ and PdO rather than PdO with lattice water, which would not react with CO.

Several reactions must occur at the surface to explain the reaction and XPS data. O_2 from the gas phase must react with CO to form CO_2 (catalytic reaction), lattice oxygen must react with CO to form CO_2 (gas-phase reaction), and surface hydroxyl groups may combine to form water, which desorbs (solid-phase reaction). Schematic diagrams of these reactions are shown in Fig. 17. No attempt is made to accurately represent the geometry or bonding structure in these schematics. The conversion data given in Figs. 4, 7, and 8 indicate that hydroxyl groups must be present for catalytic CO oxidation. This is consistent with the assertion that a bicarbonate species is the reaction intermediate, as shown in Fig. 17a. A similar mechanism was proposed for low-temperature CO oxidation over platinized tin oxide catalysts [27] based on extensive data. In this mechanism, gas-phase CO chemisorbs at a vacancy near a hydroxyl group, and gas-phase oxygen chemisorbs at a nearby vacancy to form a bicarbonate species that decomposes to yield a desorbing CO_2 molecule and two vacancies. More gas-phase CO and O_2 adsorb at these sites, and the catalytic cycle continues. Under some conditions, the bicarbonate species do not decompose rapidly, and they accumulate on the surface of supported Pt and Au catalysts, resulting in activity decay [15,36–38]. The second reaction is a gas–solid reaction in which gas-phase CO reduces Pd oxide to Pd metal (Fig. 17b). In this case, CO adsorbs near a hydroxyl group and a surface O, again forming a bicarbonate species that decomposes to a desorbing CO_2 and metallic Pd. Another pathway cannot be eliminated. In this pathway, gas-phase CO reacts with a hydroxyl group to form a surface formate intermediate that decomposes to yield a CO_2 molecule and a hydrogen that moves to another surface oxygen to form a surface hydroxyl group. The formation of metallic Pd during reaction is shown in Figs. 8–10, 11–13, and 15–17.

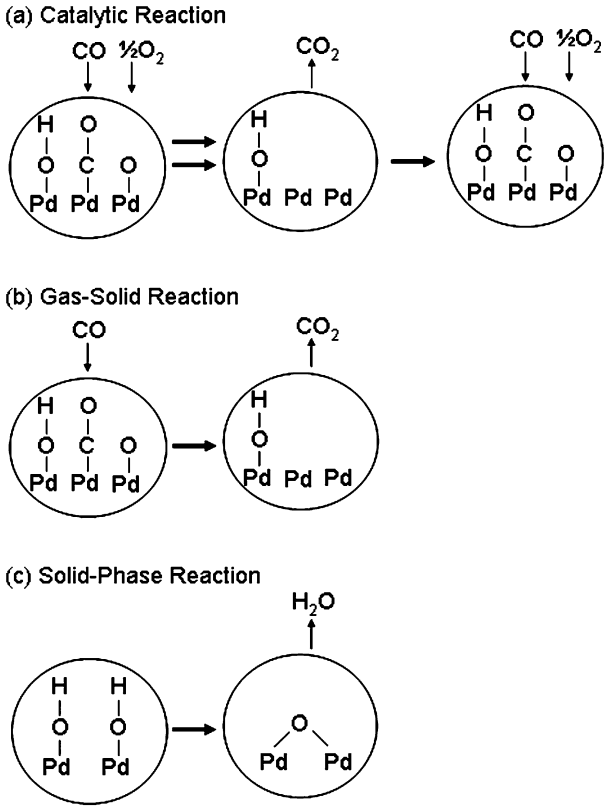

Fig. 17. Schematic diagram depicting the chemical reactions which occur over hydrous PdO during catalytic CO oxidation.

Metallic Pd is not catalytically active at these low temperatures [25], so reaction (b) results in the observed activity decay. The third reaction (c) involves reaction between two hydroxyl groups to form a water molecule that desorbs and PdO. This reaction occurs at 400 °C as shown in Figs. 4, 5, and 6. It was also observed at 150 °C (not shown). This reaction proceeds more slowly at lower temperature. Because this reaction eliminates hydroxyl groups and produces anhydrous PdO, it also contributes to activity decay. If this reaction rate is negligible at lower temperatures, then reactions (a) and (b) proceed at nearly equal rates, because the O_2 reaction rate is about one-half of the CO reaction rate. Nearly all catalysts undergo decay due to gas–solid reaction and/or solid-phase reactions. The rate of activity decay depends on the rate of these reactions. In some cases, these reactions can benefit the catalytic process, and the activity will increase with time. In the present study the gas–solid reaction is rapid, so the catalytic activity decreases rapidly.

Many studies have shown that low-temperature CO oxidation catalysts consisting of Pt, Au, or Pd supported on different oxides (noble-metal reducible oxide catalysts [39]) exhibit widely varying catalytic properties in terms of both activity and decay. This present study has shown that the activity of hydrous PdO powder decays very rapidly. Pd supported on ceria is known to be a very active catalyst for CO oxidation, more so than Pd supported on other oxides including zirconia, alumina, titania, silica, and ZSM-5. It also exhibits essentially no decay [40] even though the Pd chemical state is PdO [25]. Therefore, ceria–supported Pd is maintained in the form of PdO by accept-

ing oxygen from the ceria, which is known to have excellent oxygen storage and transfer capabilities. The activity and decay behavior of any oxide–supported Pd CO oxidation catalyst may be influenced by how rapidly oxygen is transferred from the oxide support to the supported PdO phase.

4. Conclusion

In this study, low-temperature CO oxidation was examined over hydrous PdO, anhydrous PdO that had been exposed to humid air for about 1 year, and fresh anhydrous PdO powders. The aim was to study the influence of incorporated water of hydration in PdO without the presence of support effects. XPS data indicate that the water of hydration is present as hydroxyl groups, not molecular water. During CO oxidation over hydrous PdO at 100 °C, the activity is initially high and drops to zero over time as Pd metal forms and hydroxyl groups are depleted. The oxygen required for CO oxidation originates from two sources: gas-phase and solid-phase oxygen. Fresh Ar-sealed anhydrous PdO exhibits no CO oxidation activity under these same conditions, and both hydrous PdO that had been annealed in He at 400 °C and air-exposed anhydrous PdO briefly exhibit activity that decays to zero. These results all demonstrate that the presence of hydroxyl groups is required for low-temperature CO oxidation over PdO. CO oxidation experiments carried out at 25 °C and then at 70 °C and then 100 °C with the same hydrous PdO sample indicate that subsurface hydroxyl groups migrate to the surface to maintain high activity.

During CO oxidation, three reactions occur at the surface: (1) oxidation of CO by O from PdO and hydroxyl groups, (2) oxidation of CO by chemisorbed gas-phase oxygen, and (3) formation of water, which desorbs by reaction of two hydroxyl groups, leaving PdO at the surface. A model is proposed in which reactions (1) and (2) occur through a bicarbonate intermediate.

References

[1] W.S. Epling, G.B. Hoflund, J. Catal. 182 (1999) 5.
[2] R.J. Farrauto, M.C. Hobson, T. Kennelly, E.M. Waterman, Appl. Catal. A Gen. 81 (1992) 227.
[3] H.S. Gandhi, G.W. Graham, R.W. McCabe, J. Catal. 216 (2003) 433.
[4] D.S. Stark, A. Crocker, G.J. Steward, J. Phys. E Sci. Instrum. 16 (1983) 158.
[5] D.S. Stark, M.R. Harris, J. Phys. E Sci. Instrum. 16 (1983) 492.
[6] G.C. Bond, L.R. Molloy, M.J. Fuller, J. Chem. Soc. Chem. Commun. (1975) 796.
[7] W. Ibashi, G. Groppi, P. Forzatti, Catal. Today 83 (2003) 115.
[8] M. Lyubovsky, L. Pfefferle, Catal. Today 47 (1999) 29.
[9] A.K. Datye, J. Bravo, T.R. Nelson, P. Atanasova, M. Lyubovsky, L. Pfefferle, Appl. Catal. A Gen. 198 (2000) 179.
[10] M. Haruta, T. Kobayashi, H. Sano, N. Yamada, Chem. Lett. 15 (1987) 405.
[11] M. Haruta, N. Yamada, T. Kobayashi, S. Iijima, J. Catal. 115 (1989) 301.
[12] S.D. Gardner, G.B. Hoflund, D.R. Schryer, B.T. Upchurch, E.J. Kielin, Langmuir 7 (1991) 2135.
[13] S.D. Gardner, G.B. Hoflund, D.R. Schryer, B.T. Upchurch, J. Phys. Chem. 95 (1991) 835.
[14] G.B. Hoflund, B.T. Upchurch, E.J. Kielin, D.R. Schryer, Catal. Lett. 31 (1995) 133.
[15] G.B. Hoflund, S.D. Gardner, D.R. Schryer, B.T. Upchurch, E.J. Kielin, Langmuir 11 (1995) 3431.
[16] G.B. Hoflund, S.D. Gardner, D.R. Schryer, B.T. Upchurch, E.J. Kielin, React. Kinet. Catal. Lett. 58 (1996) 19.
[17] W.S. Epling, G.B. Hoflund, J.F. Weaver, S. Tsubota, M. Haruta, J. Phys. Chem. 100 (1996) 9929.
[18] M. Daté, M. Haruta, J. Catal. 201 (2001) 221.
[19] M. Haruta, M. Date, Appl. Catal. A Gen. 222 (2001) 427.
[20] Y. Bi, G. Lu, Appl. Catal. B Environ. 41 (2003) 279.
[21] D.I. Kochubey, S.N. Pavlova, B.N. Novgorodov, G.N. Kryukova, V.A. Sadykov, J. Catal. 161 (1996) 500.
[22] H. Zhu, Z. Qin, W. Shan, W. Shen, J. Wang, J. Catal. 233 (2005) 41.
[23] B.L.M. Hendriksen, S.C. Bobaru, J.W.M. Frenken, Surf. Sci. 552 (2004) 229.
[24] G.B. Hoflund, Z.-H. Li, W.S. Epling, T. Göbel, P. Schneider, H.W. Hahn, React. Kinet. Catal. Lett. 70 (2000) 97.
[25] S.-H. Oh, G.B. Hoflund, J. Phys. Chem. A 110 (2006) 7609.
[26] S.D. Gardner, G.B. Hoflund, M.R. Davidson, D.R. Schryer, J. Catal. 115 (1989) 132.
[27] D.R. Schryer, B.T. Upchurch, B.D. Sidney, K.G. Brown, G.B. Hoflund, R.K. Herz, J. Catal. 130 (1991) 314.
[28] R.E. Gilbert, D.F. Cox, G.B. Hoflund, Rev. Sci. Instrum. 53 (1982) 1281.
[29] Th. Pillo, R. Zimmermann, P. Steiner, S. Hüfner, J. Phys. Condens. Matter 9 (1997) 3987.
[30] K. Andersson, A. Nikitin, L.G.M. Petterson, A. Nilsson, H. Ogasawara, Phys. Rev. Lett. 93 (2004), 196101-1.
[31] J.F. Moulder, W.F. Stickle, P.E. Sobol, K.D. Bowman, Handbook of X-Ray Photoelectron Spectroscopy, Physical Electronics, Eden Prairie, MN, 1995.
[32] J.E. Drawdy, G.B. Hoflund, S.D. Gardner, E. Yngvadottir, D.R. Schryer, Surf. Interface Anal. 16 (1990) 369.
[33] J.F. Weaver, G.B. Hoflund, J. Phys. Chem. 98 (1994) 8519.
[34] F.P. Leisenberger, G. Koller, M. Sock, S. Surnev, M.G. Ramsey, F.P. Metzer, B. Klötzer, K. Hayek, Surf. Sci. 445 (2000) 380.
[35] G.B. Hoflund, in: J.C. Riviere, S. Myhra (Eds.), Handbook of Surface and Interface Analysis: Methods in Problem Solving, vol. 57, Dekker, New York, 1998.
[36] M. Haruta, S. Tsubota, T. Kobayashi, H. Kageyama, M. Genet, B. Delmon, J. Catal. 144 (1993) 175.
[37] B. Schumacher, Y. Denkwitz, V. Plzak, M. Kinne, R.J. Behm, J. Catal. 224 (2004) 449.
[38] M. Azar, V. Caps, F. Morfin, J.-L. Rousset, A. Piednoir, J.-C. Bertolini, L. Piccolo, J. Catal. 239 (2006) 307.
[39] D.R. Schryer, G.B. Hoflund (Eds.), Low-Temperature CO-Oxidation Catalysts for Long-Life CO_2 Lasers, NASA Conference Publication 3076, 1990.
[40] M.-F. Luo, Z.-Y. Hou, X.-X. Yuan, X.-M. Zheng, Catal. Lett. 50 (1998) 205.